Surface Review and Letters, 2150009 (5 pages)

DOI: 10.1142/S0218625X21500098

World Scientific
www.worldscientific.com

THE EFFECT OF IRON ON THE SURFACE GRAPHITIZATION OF SILICON CARBIDE

ELIF MERCAN
İ.D. Bilkent University, Faculty of Art, Design & Architecture,
Interior Architecture and Environmental Design - Building Science

GOKNUR CAMBAZ BUKE*
Department of Materials Science and
Nanotechnology Engineering,
Micro Nanotechnology Graduate Program,
TOBB University of Economics and Technology,
Ankara, Turkey
goknurcambaz@gmail.com

Received 22 June 2020
Revised 3 December 2020
Accepted 6 December 2020
Published 6 January 2021

In order to decrease the decomposition temperature of SiC, 12 nm Fe thin film is applied on SiC substrates as a catalyst layer using electron beam (e-beam) deposition. To investigate the mechanism of Fe-treated SiC decomposition, local Fe regions are formed through dewetting of the catalyst layer by hydrogen annealing. The results show that Fe decreases the decomposition temperature of SiC effectively and increases the kinetics of the graphitization. Studies showed that depending on the amount of Fe, crumpled and ordered graphene films can be synthesized simultaneously on SiC by using this method.

Keywords: Graphene; silicon carbide; iron; hydrogen; graphitization.

1. Introduction

Ever since the graphene was first isolated and its extraordinary properties were shown, various applications have been proposed for it. Among the alternative methods, the high temperature-vacuum annealing of SiC has been an attractive route for controlled, continuous and high-quality graphene leading to wafer size material for large-scale device production.[1,2] In this process, Si atoms are sublimated from the surface selectively and the remaining surface C atoms rearrange to form graphene on the surface.[3] However, temperatures exceeding 1500°C are required to form high-quality graphene[4] in this method. With respect to that, recently a catalyst-based method was developed for obtaining graphene on SiC at lower temperatures.

Catalyst-based SiC decomposition method involves depositing a thin metallic film that reacts with SiC and releases the carbon in SiC. The decomposition of SiC by various transition metals,[5] Co,[6–9] alloy systems[10–12] and Ni in particular,[13–16] has

*Corresponding author.

been reported. Iron mediated growth of epitaxial graphene has also been studied and it is shown that 1–3 nm is sufficient to initiate the graphitization.[17] In those studies, mostly the metallic film on the surface is kept continuous and carbon formation is aimed to be understood by investigating the surface and the interface between SiC and the metallic thin film.

In this study, in order to investigate the mechanism of Fe-treated SiC decomposition, we formed local regions with Fe islands by dewetting of the catalyst layer. The dewetting is a well-known phenomenon and mostly used to prepare catalyst nanoparticles for 1D nanomaterial growth (such as nanowires, nanotubes, nanorods, etc.). Since the thin film deposited on a substrate is mostly a metastable phase, it forms islands, i.e. dewetting occurs in hydrogen atmosphere at different temperatures for various metal-substrate systems.[18] Therefore in this study, Fe-treated SiC samples are annealed in hydrogen and the surface morphology is characterized after the processes in detail in order to understand the effect of Fe on SiC decomposition.

2. Experimental

In this study, 0.5 mm thick single crystal 4H-SiC wafer (from Cree Inc.) was used. The carbon terminated face of the SiC substrate was first cleaned using ethanol and 12 nm thick iron film was applied using e-beam deposition method. Substrates with thin films were then placed in a quartz tube furnace connected to Ar, H_2 (with Mass Flow Controllers) and a rotary pump; and heated to 800°C and 1100°C in Ar/H_2 (50/15 sccm) and annealed at those temperatures in the same gas composition for 30 minutes. After annealing, all the gases were stopped and the system was cooled down to room temperature in vacuum (10^{-3} Torr). Surface morphologies of the samples were characterized using SEM, EDAX, Raman spectroscopy and XPS. In order to remove the oxides and Fe compounds that form on the surface, the samples were dipped in $HF:HNO_3:H_2O$ (1: 1: 2) acid solution.

3. Results and Discussion

The surface morphologies of the 12 nm coated SiC samples after hydrogen annealing at 800°C and 1100°C are given in Fig. 1. The Fe islands formed on the surface as a result of dewetting are homogeneously distributed on the surface (Figs. 1(a) and 1(b)). On the other hand, Fig. 1(d) shows that annealing at 1100°C results in the formation of three regions: light crumpled structures sitting on the

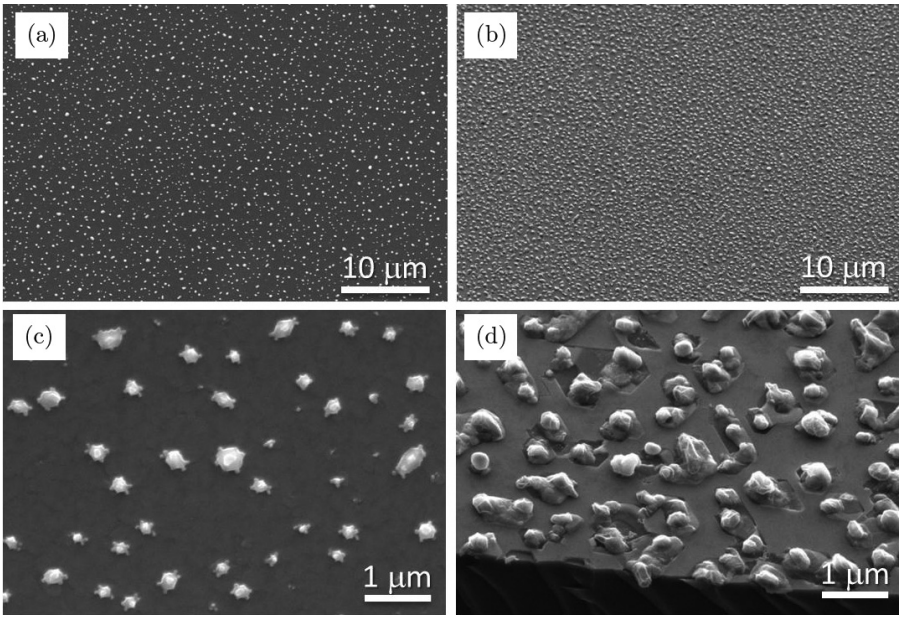

Fig. 1. Lower and higher magnification SEM images of the surface morphology of 12 nm Fe coated SiC C-face after (a), (b) 800°C and (c), (d) 1100°C hydrogen annealing.

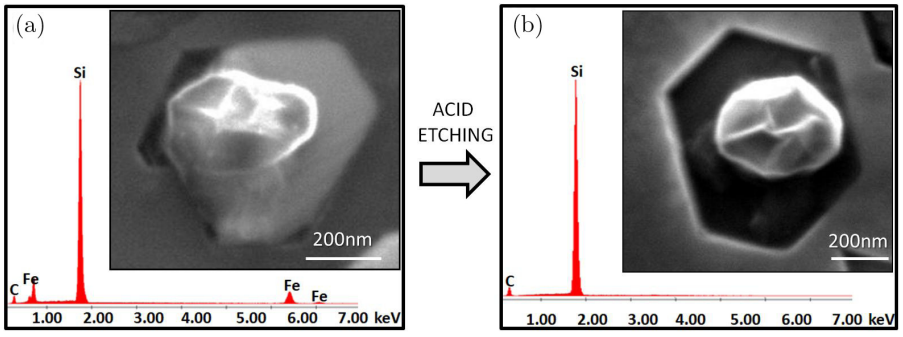

Fig. 2. (Color online) The effect of acid treatment on substrates coated by electron beam and annealed with hydrogen at high temperature: (a) SEM image and EDX results of the sample annealed with hydrogen for 30 min at 1100°C after 12 nm Fe coating, (b) SEM image and EDX results of the same sample after acid treatment.

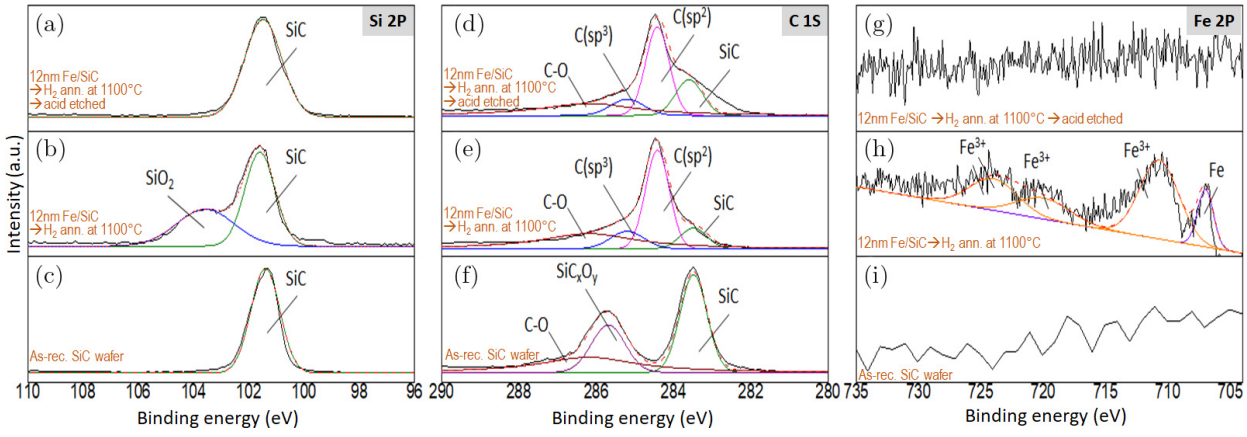

Fig. 3. (Color online) (a)–(c) Si2p, (d)–(f) C1s and (g)–(i) Fe2p core level sectra for as-received SiC, 12 nm Fe coated SiC which is hydrogen annealed at 1100°C, and acid etched sample.

faceted pits (mentioned with the arrows in Fig. 1(d)), fuzzy light phases around the crumpled structures, and smooth flat surface. These regions are considered to be the Fe-island regions shown in Fig. 1(b). Hence, it shows that the presence of Fe decreases the SiC decomposition temperature and increases the graphitization rate which results in the formation of different carbon morphology.

In order to selectively remove the iron compounds and oxides, the sample was dipped into acid solution. Figure 2 shows that the fuzzy phase around the crumpled structure is removed completely after etching; and the crumpled structure is left on the pits. EDS studies before and after etching showed that the fuzzy phase is mostly the iron compound (Fig. 2).

To understand the mechanism further, XPS studies were performed on three samples: as-received

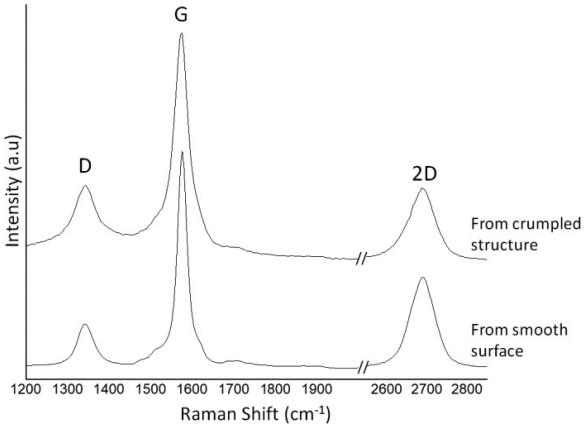

Fig. 4. Raman spectroscopy results obtained from the surface and the crumpled structure of the sample annealed with hydrogen at high temperature after electron beam deposition, after acid etching.

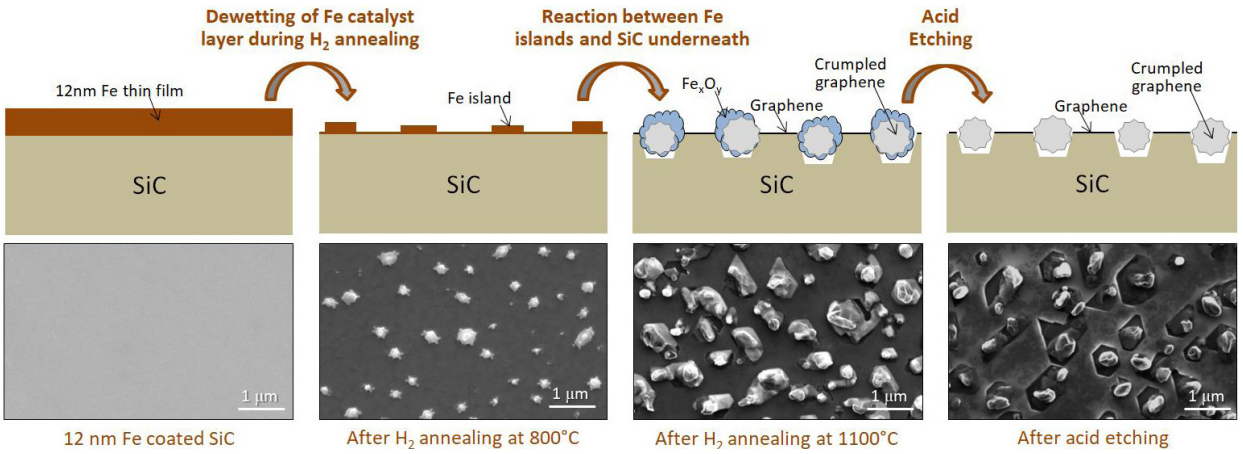

Fig. 5. (Color online) Upper row shows the (cross-sectional) schematic drawing of the steps during process; Lower row shows the SEM images (top view) of the relevant surfaces.

SiC, 12 nm Fe coated SiC which was hydrogen annealed at 1100°C, and third one is the second's acid etched version (Fig. 3). After the hydrogen annealing, SiO_2, Fe_xO_y, and carbon (sp2 and sp3) formation are recorded (Figs. 3(b), 3(e), and 3(h)). These oxide formations are attributed to the presence of oxygen in the system. As mentioned above, during process, the oxidation is lowered by passing Ar/H_2 (50/15 sccm) through the furnace and the system was cooled down in low vacuum (10^{-3} Torr) by using rotary pump. Hence, this is not sufficient to completely prevent the oxidation. XPS studies confirm that the acid etching removes the Fe_xO_y and SiO_2 selectively leaving behind the carbon (Fig. 3).

Raman studies were also performed to characterize the two types of carbon formed on the surface. Raman spectra taken from the smooth surface and crumpled structure after etching confirm that they are both graphitic (Fig. 4). D and G band (I(D)/I(G)) ratios for crumpled structure and the graphene formed on smooth surface are found to be 0.31 and 0.19, respectively.

The steps of the process and the resulting structures formed using this new approach are shown schematically in Fig. 5. According to this, during hyrogen annealing, Fe thin film first dewets and forms Fe islands on the SiC surface. At higher temperatures (1100°C), Fe islands react with the SiC underneath, forming carbon. This is in parallel with literature because Fe-SiC phase diagram[19,20] shows that when there is enough Fe in the system, Fe catalyzes the formation of carbon. Since the Fe atoms are concentrated on the formed Fe islands, SiC decomposition is accelerated under these regions, which results in formation of more free carbon and finally crumpled graphene.

4. Conclusions

In this study, in order to investigate the effect of Fe on SiC decomposition, Fe islands were formed on SiC wafer by using the dewetting phenomenon of the catalyst layer. Our results show that Fe island/SiC regions transform into crumpled graphitic structures and Fe compound (which then can be etched by acid) in a faceted pit. As a result, it is shown that the Fe decreases the decomposition temperature of SiC effectively and increases the kinetics of graphitization. By controlling the processing parameters further (catalyst layer thickness, annealing temperature, duration and atmosphere), one can use this technique to synthesize a controlled hybrid structure of crumpled graphene together with continuous flat graphene.

Acknowledgment

This work was supported by TUBITAK (Grant No. 213M481).

References

1. K. V. Emtsev, A. Bostwick, K. Horn, J. Jobst, G. L. Kellogg, L. Ley, J. L. McChesney, T. Ohta, S. A.

Reshanov, J. Röhrl, E. Rotenberg, A. K. Schmid, D. Waldmann, H. B. Weber and T. Seyller, *Nat. Mater.* **8** (2009) 203, doi: 10.1038/nmat2382.
2. A. Ouerghi, M. G. Silly, M. Marangolo, C. Mathieu, M. Eddrief, M. Picher, F. Sirotti, S. El Moussaoui and R. Belkhou, *ACS Nano.* **6** (2012) 6075, doi: 10.1021/nn301152p.
3. Z. G. Cambaz, G. Yushin, S. Osswald, V. Mochalin and Y. Gogotsi, *Carbon N. Y.* **46** (2008) 841, doi: 10.1016/j.carbon.2008.02.013.
4. B. L. VanMil, R. L. Myers-Ward, J. L. Tedesco, C. R. Eddy Jr., G. G. Jernigan, J. C. Culbertson, P. M. Campbell, J. M. McCrate, S. A. Kitt and D. K. Gaskill, *Mater. Sci. Forum.* **615–617** (2009) 211, doi: 10.4028/www.scientific.net/MSF.615-617.211.
5. M. Backhaus-Ricoult, *Acta Met. Mater.* **40** (1992) s95.
6. P. Macháč, T. Fidler, S. Cichoň and V. Jurka, *J. Mater. Sci. Mater. Electron.* **24** (2013) 3793, doi: 10.1007/s10854-013-1320-1.
7. P. Macháč, S. Cichoň, L. Mišková and M. Vondráček, *Appl. Surf. Sci.* **320** (2014) 544, doi: 10.1016/j.apsusc.2014.09.104.
8. P. Machac and T. Hrebicek, *J. Mater. Sci. Mater. Electron.* **28** (2017) 12425, doi: 10.1007/s10854-017-7063-7.
9. C. Li, D. Li, J. Yang, X. Zeng and W. Yuan, *J. Nanomater.* **2011**, 319624 (2011), doi: 10.1155/2011/319624.
10. E. Escobedo-Cousin, K. Vassilevski, T. Hopf, N. Wright, A. Oneill, A. Horsfall, J. Goss and P. Cumpson, *J. Appl. Phys.* **113** (2013) 114309, doi: 10.1063/1.4795501.
11. F. Iacopi, N. Mishra, B. V. Cunning, D. Goding, S. Dimitrijev, R. Brock, R. H. Dauskardt, B. Wood and J. Boeckl, *J. Mater. Res.* **30** (2015) 609, doi: 10.1557/jmr.2015.3.
12. N. Mishra, J. J. Boeckl, A. Tadich, R. T. Jones, P. J. Pigram, M. Edmonds, M. S. Fuhrer, B. M. Nichols and F. Iacopi, *J. Phys. D. Appl. Phys.* **50** (2017) 95302, doi: 10.1088/1361-6463/aa560b.
13. Z. Y. Juang, C. Y. Wu, C. W. Lo, W. Y. Chen, C. F. Huang, J. C. Hwang, F. R. Chen, K. C. Leou and C. H. Tsai, *Carbon N. Y.* **47** (2009) 2026, doi: 10.1016/j.carbon.2009.03.051.
14. A. A. Woodworth and C. D. Stinespring, *Carbon N. Y.* **48** (2010) 1999, doi: 10.1016/j.carbon.2010.02.007.
15. J. Hofrichter, B. N. Szafranek, M. Otto, T. J. Echtermeyer, M. Baus, A. Majerus, V. Geringer, M. Ramsteiner and H. Kurz, *Nano Lett.* **10** (2010) 36, doi: 10.1021/nl902558x.
16. A. Delamoreanu, C. Rabot, C. Vallee and A. Zenasni, *Carbon N. Y.* **66** (2014) 48, doi: 10.1016/j.carbon.2013.08.037.
17. S. P. Cooil, F. Song, G. T. Williams, O. R. Roberts, D. P. Langstaff, B. Jørgensen, K. Høydalsvik, D. W. Breiby, E. Wahlström, D. A. Evans and J. W. Wells, *Carbon N. Y.* **50** (2012) 5099, doi: 10.1016/j.carbon.2012.06.050.
18. M. V. Putz and O. Ori, *Book Series: Carbon Materials-Chemistry and Physics* **8**, V (2015), doi: 10.1007/978-94-017-9567-8.
19. S. C. Chueh and J. F. Smith, *Comput. Coupling Phase Diagrams Thermochem.* **11** (1987) 149.
20. Y. G. Timoshenko and M.P. Gadzyra, Powder Metall. Met Ceram., 51, No. 5–6, 295–300 (2012), https://doi.org/10.1007/s11106-012-9431-4..